PHYSICAL REVIEW C VOLUME 32, NUMBER 3 SEPTEMBER 1985

Diffraction theory analysis of pion elastic scattering from the calcium isotopes

Jean-François Germond
Institut de Physiqué, Neuchâtel, Switzerland

Mikkel B. Johnson and John A. Johnstone*
Los Alamos National Laboratory, Los Alamos, New Mexico 89544
(Received 13 May 1985)

We show that the experimental results for pion elastic scattering from the calcium isotopes in the Δ_{33} resonance region can be well represented at small angles in terms of the variables of diffraction theory. The parameters describing the amplitude reflect physics that can be attributed to pion and Δ_{33} dynamics in a microscopic approach, as well as to details of the neutron and proton densities. Using a phenomenological determination of the former, we show that the expermental results require a neutron skin in excess of that obtained from scaling the proton density according to the relative number of neutrons and protons. The experimental results are consistent with microscopic Hartree-Fock densities, provided that the ratio of isovector to isoscalar optical potential is substantially enhanced over the value obtained from the free pion-nucleon scattering amplitude. The size of this enhancement agrees with pion single-charge-exchange scattering from the calcium isotopes.

I. INTRODUCTION

Pion-nucleus scattering in the resonance region presents two superficially contradictory appearances. On the one hand, the interaction appears to be a complicated process whose essential features are determined by an interplay between various nonlocalities, isobar-hole collective states, and a variety of interesting many-body effects. These intricacies are most pronounced at the energies for which the pion couples most strongly to elementary pion-nucleon resonances, for example the Δ_{33} at a pion laboratory energy of about 180 MeV. In the last few years a great deal of theoretical effort has been directed toward the development of microscopic models that incorporate these effects.[1–8]

On the other hand, the pion-nucleon amplitude is very strong in the region of the Δ_{33} resonance. The combination of a strongly absorptive interaction with a short wavelength projectile suggests that the scattering process displays a dominantly geometrical character and therefore that the appropriate variables are those of diffraction theory. Indeed, some of the earliest successful attempts to represent pion elastic scattering[9] involved the use of Glauber's theory.[10]

Of course, one is not faced with choosing between two incompatible alternatives, but rather deciding upon the most convenient set of variables to answer the questions being asked. In order to decide which representation is appropriate it is important to have a detailed understanding of the transformation between the two sets of variables. In this paper we examine how well the semiclassical theory represents elastic scattering and interpret the results in terms of a more microscopic theory. One of our main interests is to study the sensitivity of the cross sections to the choice of neutron and proton densities. The semiclassical theory is appropriate for this purpose because it faithfully reproduces the sensitivity of the underlying theory to changes in the neutron and proton densities and because much of the study can be carried out analytically.[11]

An analysis of neutron densities in the calcium isotopes based on pion scattering data was made earlier in Refs. 12–14. The present analysis is similar to that of Ref. 13, but is different in that we use a more refined version of the analytical theory[11] (described in Sec. II). In Sec. III we apply this theory to the extensive data set of Ref. 15 for 180-MeV $\pi^{\pm}$ elastic scattering from ^{40}Ca, ^{42}Ca, ^{44}Ca, and ^{48}Ca. Interpretation of the semiclassical analysis is given in Sec. IV. In Sec. V we examine the sensitivity to neutron densities and show the relevance of the pion single-charge-exchange (SCX) data[16] at 180 MeV from ^{42}Ca, ^{44}Ca, and ^{48}Ca. Justification of this analysis is based on recent results[17] that show a simple, universal scaling of the optical potential throughout the periodic table in terms of a few phenomenologically determined parameters.

II. ANALYTICAL THEORY

During the past few years it has been recognized by several groups that diffraction theory for elastic scattering has a very simple analytical representation in both the low- (Refs. 11, 13, and 18) and high-momentum[19,20] transfer regions, and that only a few physically meaningful parameters are needed to characterize the amplitude. The analytical form of diffraction theory has been successfully applied to proton-nucleus scattering.[20] In this section we wish to discuss the theory that we will apply to pion scattering in Sec. III; the results quoted are discussed more fully in Ref. 11.

In the absence of the Coulomb interaction the differential cross section for elastic scattering is given by

$$\frac{d\sigma}{d\Omega}=|F(\theta)|^2\,, \tag{1}$$

where, in the eikonal approximation,

$$F(\theta)=ikR\frac{J_1(qR)}{q}G(q) \tag{2}$$

and

$$G(q)=\cos\sigma_0(qa)\frac{\pi qa}{\sinh\pi qa} . \tag{3}$$

The amplitude has the well-known form of diffractive scattering of a fuzzy black disk of radius R. The quantity $G(q)$ is the "Inopin factor"[21] that damps the oscillations of the cross section at large momentum transfer, which is required when the edge of the disk is not sharp but is spread out over a distance a. The quantity $\sigma_0(qa)$ is given by

$$e^{2i\sigma_0(qa)}=\frac{\Gamma(1+iqa)}{\Gamma(1-iqa)} . \tag{4}$$

The quantity R in Eq. (2) has a weak dependence on momentum transfer, which is approximately

$$R(q)=R(0)-0.337a(qa)^2 . \tag{5}$$

For nuclei as large as calcium, the dependence on q may be ignored in practice. The quantity $R(0)$ is complex, which means that the real and imaginary amplitudes will fall off with q at different rates. When the Coulomb interaction is included, the expressions are slightly more complicated.[11]

In Sec. III we show how well the analytical expressions for the amplitude represent the $\pi^{\pm}$ scattering data. Rather than tabulating $R(0)$ and a we give instead the set of parameters a, b_1, and Y, which are related to $R(0)$ by

$$R^2(0)=\{b_1+a[0.211+\tfrac{1}{2}\ln(1+Y^2)-i\tan^{-1}Y]\}^2 + 1.645a^2 . \tag{6}$$

The importance of a, b_1, and Y is that they are related to the optical potential U in a very direct manner. The equation

$$|\exp i\chi(b_1)|=\tfrac{1}{2} \tag{7}$$

determines b_1, around which $\chi(b)$ is given by

$$\chi(b)=-\frac{1}{2k}\int_{-\infty}^{\infty}U(\sqrt{b^2+z^2})dz$$
$$\cong-(2\pi a_0 b)^{1/2}U(b)/2k \tag{8}$$

and where $U(b)$ is assumed to behave like

$$U(b)=U(b_1)e^{(b_1-b)/a_0} \tag{9}$$

in a small region of the nuclear surface for $b\approx b_1$. The quantities a and Y are then

$$a=-\frac{\chi(b_1)}{\chi'(b_1)}\cong a_0\left[1-\frac{a_0}{2b_1}\right]^{-1} \tag{10}$$

and

$$Y=\frac{\mathrm{Re}\chi(b_1)}{\mathrm{Im}\chi(b_1)}=\frac{\mathrm{Re}U(b_1)}{\mathrm{Im}U(b_1)} . \tag{11}$$

When the Coulomb residual interaction is taken into account, Eqs. (7) and (8) are changed[22] by setting

$$b_1\rightarrow b_1[1+EV_C(b_1)/k^2]\equiv\tilde{b}_1 \tag{12}$$

to account for the focusing of the pions by the Coulomb field, and setting

$$E\rightarrow E-V_C(b_1) \tag{13}$$

to take account of the fact that the pion kinetic energy is changed in the nucleus by the long-range Coulomb interaction.

The parameters a, b_1, and Y have unambiguous geometrical interpretations. The quantity b_1 locates the size of the diffractive disk, which determines the frequency of the oscillation pattern of the angular distribution. The quantity Y determines the relative real part of the scattering amplitude, which is most sensitive to the depths of the minima of the angular distribution. Finally, a determines the rate of falloff of the angular distribution through the Inopin factor in Eq. (3). In order to obtain numerical values for a, b_1 and Y from the data, the angular distribution should be accurately measured for q extending to at least the position of the first secondary maximum.

III. FIT TO ELASTIC SCATTERING

An impressive data set for $\pi^{\pm}$ elastic scattering from the calcium isotopes has been taken with the EPICS spectrometer at LAMPF.[15] We have fit these data with the parameters a, b_1, and Y discussed in Sec. II. The version of the theory we used incorporated the form of scattering amplitude involving the Coulomb interaction. We tried to get the best fit possible over the momentum-transfer range out to the position of the second minimum ($qb_1 \lesssim 2\pi$, corresponding to $\theta\lesssim 55°$ for ^{40}Ca). The results of the fit are given in Fig. 1 for π^+ and Fig. 2 for π^-. The data beyond 55° are not reproduced because they were not included in the least-squares fit.

We fit the data for $\theta\lesssim 55°$ only in order to establish as accurately as possible the location of the first diffraction minimum which, as discussed, then gives an accurate value for b_1. The systematics of this feature of the data reflects the details of the variation of neutron and proton densities in the nuclear surface.

The best-fit parameters obtained from the analysis of the EPICS data[15] at 180 MeV are given in Table I. Parameters obtained from the analysis of the SIN data on ^{40}Ca and ^{48}Ca at the same energy can be found in Ref. 14. Both sets of parameters are compatible within experimental errors. For simplicity our analysis is based on the values quoted in Table I. In the Secs. IV and V we give a detailed discussion of their meaning.

We close this section by giving a table of the forward scattering amplitude that would be measured in transmission experiments or careful Coulomb-nuclear (CN) interference measurements.[23] When the Coulomb interaction is included, the scattering amplitude may be written

$$F(\theta)=F_{\mathrm{pt}}(\theta)+F_{\mathrm{CN}}(\theta) , \tag{14}$$

where F_{pt} is the point Coulomb amplitude. The empirical results for $\mathrm{Re}F_{\mathrm{CN}}(0)$ and $\mathrm{Im}F_{\mathrm{CN}}(0)$ are given in Table II.

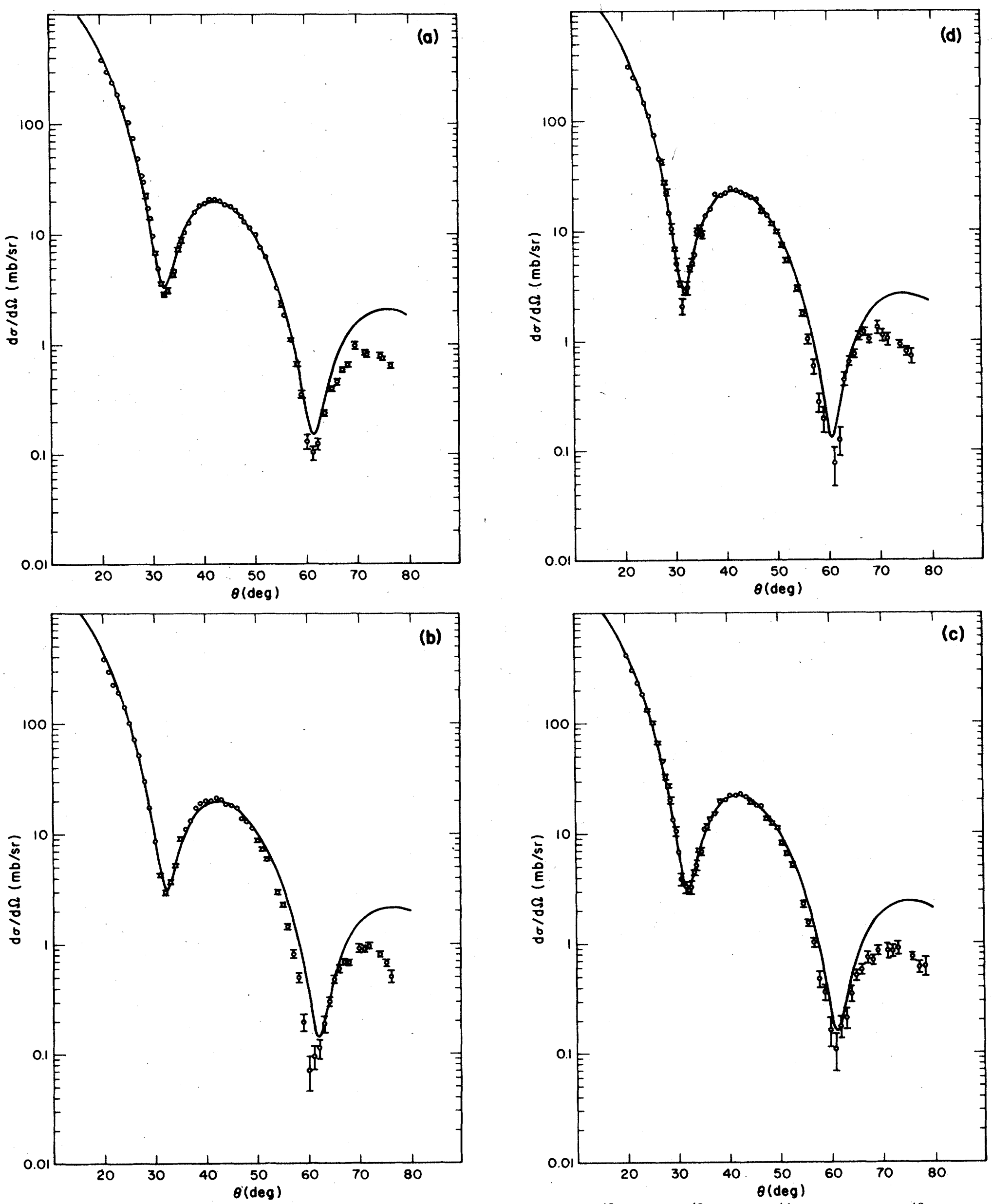

FIG. 1. Elastic scattering of π^+ mesons from the calcium isotopes. (a) ^{40}Ca, (b) ^{42}Ca, (c) ^{44}Ca, and (d) ^{48}Ca. The data are from Ref. 15(a). The solid curves are fits of the analytical theory to the data.

TABLE I. Best-fit parameters for $\pi^{\pm}$ elastic scattering from calcium isotopes obtained from the data of Ref. 15 at 180 MeV. Quoted errors are purely statistical.

Isotope	Pion	b_1 (fm)	a (fm)	Y
^{40}Ca	π^-	4.731±0.002	0.717±0.002	−0.118±0.006
	π^+	4.640±0.001	0.661±0.002	−0.112±0.003
^{42}Ca	π^-	4.819±0.003	0.720±0.003	−0.092±0.007
	π^+	4.671±0.003	0.680±0.003	−0.116±0.005
^{44}Ca	π^-	4.893±0.004	0.700±0.004	−0.099±0.013
	π^+	4.687±0.003	0.648±0.004	−0.113±0.005
^{48}Ca	π^-	5.002±0.004	0.645±0.005	−0.088±0.013
	π^+	4.715±0.003	0.627±0.004	−0.093±0.005

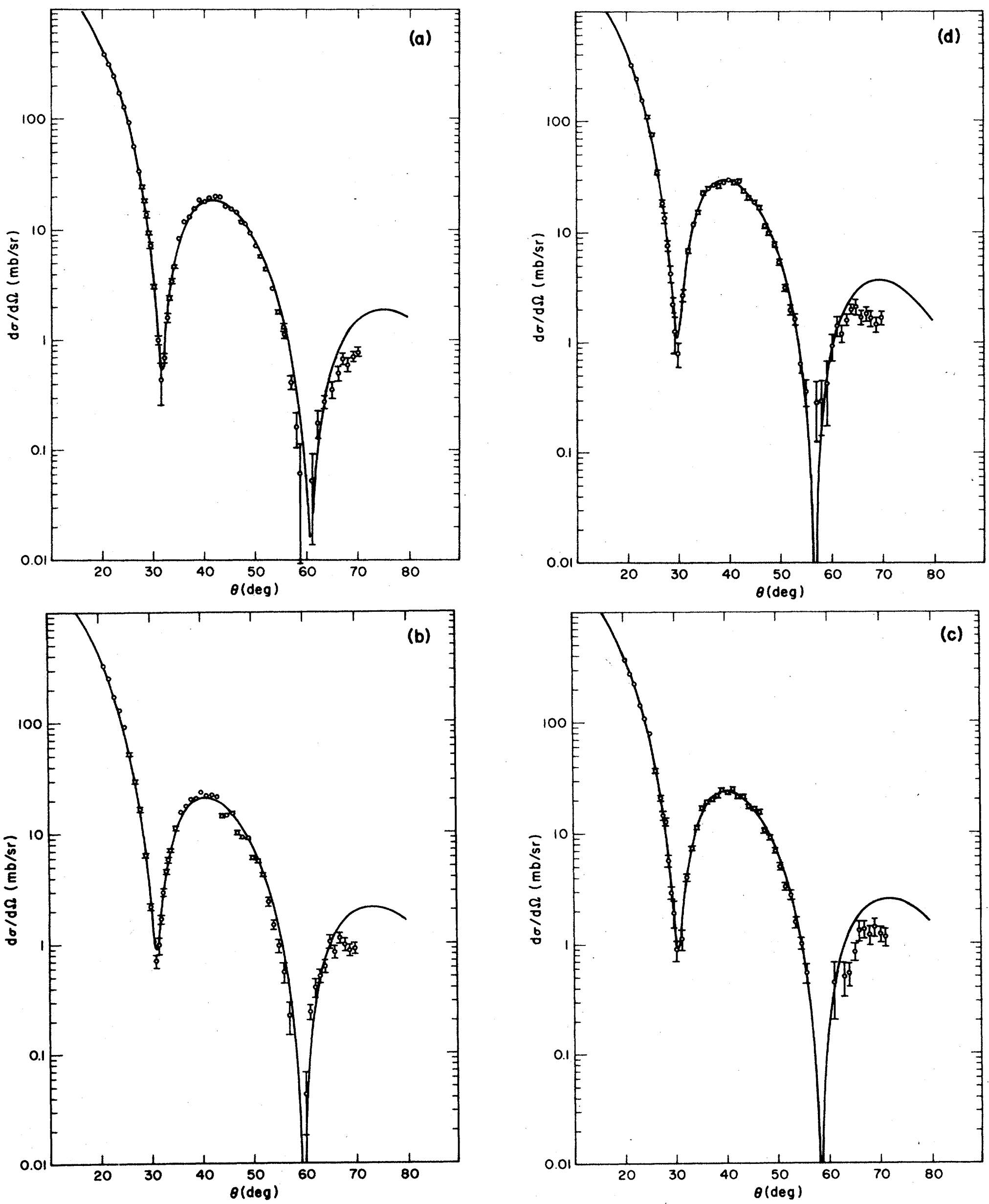

FIG. 2. Elastic scattering of π^- mesons from the calcium isotopes. (a) ^{40}Ca, (b) ^{42}Ca, (c) ^{44}Ca, and (d) ^{48}Ca. The data are from Ref. 15(a). The solid curves are fits of the analytical theory to the data.

TABLE II. Values of forward-scattering amplitude (in fm) at 180 MeV.

		Forward amplitude		Transmission experiment[a]	
Isotope	Pion	Re$F_{\mathrm{CN}}(0)$	Im$F_{\mathrm{CN}}(0)$	Re$F_{\mathrm{CN}}(0)$	Im$F_{\mathrm{CN}}(0)$
^{40}Ca	π^-	8.0	15.8	4.9±1.6	18.8±1.3
	π^+	−8.4	14.5	−7.8±1.7	14.8±1.4
^{42}Ca	π^-	8.5	16.3		
	π^+	−8.6	14.7		
^{44}Ca	π^-	8.7	16.7		
	π^+	−8.5	14.8		
^{48}Ca	π^-	9.1	17.2		
	π^+	−8.5	15.0		

[a]Interpolated from Ref. 24.

TABLE III. Total cross section differences (in mb).

Isotopes	Pion	Fit to elastic $\Delta\sigma_T$	Transmission experiment[a] $\Delta\sigma_T$
^{48}Ca-^{40}Ca	π^+	36	30±13
	π^-	150	160±12
^{44}Ca-^{40}Ca	π^+	25	13±13
	π^-	96	100±12

[a]Reference 12.

We have not given the Coulomb-corrected amplitude, which is easily obtained[11] by setting the Coulomb parameter η to zero, because we believe that there may be other effects of the Coulomb interaction not accounted for in this procedure. The results for ^{40}Ca are compared to recent LAMPF total cross-section data.[24] One sees that the values are in agreement, which implies among other things that the variation of Re$F(q)$ with q is given correctly in the theory. Table III gives our empirical values for the differences between total cross sections on the calcium isotopes. They are within error bars of the transmission data of Ref. 12.

IV. INTERPRETATION

We have shown that the analytical theory reproduces quite well the details of the angular distribution from zero degrees out to the position of the second maximum of the differential cross section. Thus the quantities b_1, a, and Y carry most of the detailed information content of the data. In this section we study these quantities based on the optical model theory of Ref. 5, which includes important dynamical effects arising at the level of second order in density. Some of the gross features of the data can be understood without the second-order dynamical effects, and so we first examine the adequacy of the lowest-order theory.

In order to relate the optical model to the eikonal results, it is necessary to cast the nonlocal potential[5] into an equivalent local form. The result of doing this, including second-order terms, is given in Ref. 5(b) and this equivalent lowest-order potential has the form

$$U(r)=-k^2\left[\left\{\bar{\lambda}_0^{(1)}+\lambda_0^{(1)}\left[1+\frac{p_1}{2k^2}\frac{\nabla^2\rho(r)}{\rho(r)}\right]\right\}\rho(r)-\epsilon_\pi\left\{\bar{\lambda}_1^{(1)}+\lambda_1^{(1)}\left[1+\frac{p_1}{2k^2}\frac{\nabla^2\Delta\rho(r)}{\Delta\rho(r)}\right]\right\}\Delta\rho(r)\right], \tag{15}$$

where $\epsilon_\pi=\pm\frac{1}{2}$ for $\pi^\pm$, respectively, and where

$$\rho(r)=\rho_n(r)+\rho_p(r)\ , \tag{16a}$$

$$\Delta\rho(r)=\rho_n(r)-\rho_p(r)\ . \tag{16b}$$

The λ parameters are related to the free pion-nucleon scattering amplitude by

$$k^2\bar{\lambda}_0^{(1)}=4\pi p_1 b_0,\quad k^2\bar{\lambda}_1^{(1)}=8\pi p_1 b_1\ ,\qquad \lambda_0^{(1)}=\frac{4\pi}{p_1}c_0,\ \text{ and }\ \lambda_1^{(1)}=\frac{8\pi}{p_1}c_1 \tag{17}$$

with b_0, b_1, c_0, and c_1 related to the free pion-nucleon scattering amplitude $f_{\pi N}$ by[25]

$$f_{\pi N}=b_0+b_1\boldsymbol{\phi}\cdot\boldsymbol{\tau}+(c_0+c_1\boldsymbol{\phi}\cdot\boldsymbol{\tau})\mathbf{k}'\cdot\mathbf{k}\ , \tag{18}$$

where $\boldsymbol{\phi}$ and $\boldsymbol{\tau}$ are, respectively, the pion and nucleon isotopic spin operators. The quantity p_1 in Eqs. (15) and (17) arises from the frame transformation from the pion-nucleon to pion-nucleus center-of-mass system, and it is given by

$$p_1=(1+\omega_\pi/M)/(1+\omega_\pi/AM)\ , \tag{19}$$

where ω_π is the pion laboratory energy and M the nucleon mass.

The Wallace correction,[26] which is needed to improve the correspondence between the eikonal theory and the solution of the Klein-Gordon equation, may be included as a correction to either χ or U. The Wallace correction is particularly important in order to understand the quantity Y. In this paper we add $\delta\chi_w$ perturbatively, i.e., evaluated at an average value $\bar{b}$ of b. As a correction to χ,

$$\chi(b)\rightarrow\chi(b)+\delta\chi_w(\bar{b})\ , \tag{20}$$

it has the form

$$\delta\chi_w(b)=\frac{1}{8k^3}\int_{-\infty}^{\infty}\left[\frac{m_\pi}{\omega_\pi}U^2(b,z)+\frac{b^2}{r^2}\frac{d}{dr}U^2(b,z)\right]dz\ . \tag{21}$$

As a correction to U, the Wallace correction may be expanded in powers of ρ and $\Delta\rho$ and has the same distinctive dependence[5(b)] on these quantities as the dynamical second-order terms in U. The resulting set a, b_1, and Y leads to a scattering amplitude that agrees well with the exact solution of the Klein-Gordon equation.[11]

Consider first the case of ^{40}Ca. For this nucleus $N=Z$, and the Coulomb repulsion among protons is responsible for pushing the Hartree-Fock proton density outward at the surface slightly beyond the neutrons. One might therefore expect the angular distribution for π^+ to be more compressed than that for π^-, since the target is more spread out. A careful comparison of Figs. 1(a) and 2(a) shows that just the opposite is true empirically [this is also easily seen in Table I, where $b_1(\pi^+)<b_1(\pi^-)$]. Furthermore, we see that the larger value of b_1 (for π^-) corresponds to the smaller value of a. Because the density falls more rapidly for large r, this is also opposite to what one would naively expect.

TABLE IV. Coulomb-corrected impact parameters and values of a compared to theory.

Isotope	Pion	b_1 (exp)	$\tilde{b}_1$[a]	$\tilde{b}_1$[b]	a (exp)	$a(b_1)$[c]
^{40}Ca	π^+	4.64	4.75	4.92	0.66	0.68
	π^-	4.73	4.62	4.84	0.72	0.71
^{42}Ca	π^+	4.67	4.78	4.99	0.68	0.68
	π^-	4.82	4.71	4.92	0.72	0.78
^{44}Ca	π^+	4.69	4.80	5.02	0.65	0.67
	π^-	4.89	4.78	5.00	0.70	0.69
^{48}Ca	π^+	4.72	4.83	5.12	0.63	0.66
	π^-	5.00	4.89	5.14	0.65	0.68

[a]Trajectory correction in Eq. (12) applied to b_1(exp).
[b]Solution of Eq. (7) with lowest order U, Coulomb energy shift included.
[c]Diffuseness at radius determined from calculation b.

One can understand these trends as an effect of the Coulomb interaction in the scattering.[22,27] Because the Coulomb repulsion bends the π^+ classical trajectory away from the nucleus, the effective impact parameter increases by an amount given quantitatively in Eq. (12). For ^{40}Ca we find, taking $\langle b_1 \rangle = 4.69$ fm,

$$1+\frac{EV_C(b_1)}{k^2}=1.024 . \tag{22}$$

Thus for π^+ scattering, the amplitude becomes sensitive to the diffuseness at a radius (see Table IV)

$$\tilde{b}_1(\pi^+)=4.75 \text{ fm} . \tag{23}$$

Similarly, for π^- we find

$$\tilde{b}_1(\pi^-)=4.62 \text{ fm} . \tag{24}$$

We see now that the π^+ probes properties of the optical potential at a radius slightly larger than that of the π^-, which is what one would expect intuitively if the protons in ^{40}Ca extend beyond the neutrons as in the Hartree-Fock theory. If we compare the diffuseness at these radii, using Eq. (10) and numerically differentiating the density matrix expansion (DME) Hartree-Fock densities,[28] we find

$$a(\pi^+)=0.696 \text{ fm} . \tag{25}$$

Similarly, we find

$$a(\pi^-)=0.692 \text{ fm} . \tag{26}$$

These values are both close to the empirical results of 0.66 and 0.72 fm, respectively.

We thus see that some of the mixing of the strong interaction with the Coulomb interaction is well understood. In addition to this Coulomb effect, there is the modification in Eq. (13) that is less well understood and discussed in connection with Figs. 3 and 4 below.

Consider now the extent to which the values of b_1 in Table I are compatible with the lowest order U, which is given as the solution of Eqs. (7)–(11) and (15)–(21). We have solved these equations using the DME theory[28] for $\rho_n(r)$ and $\rho_p(r)$ and give the results in Table IV. From this table it is evident that the difference δ between the b_1 values of the lowest-order optical potential and the data is $\delta \approx 0.25$ fm. This corresponds to a relative displacement of the minima in $d\sigma/d\Omega$ by an angle of $\Delta\theta \simeq 1.5°$. A similar feature was found by Zeidman[29] in his study of the calcium isotopes based on a numerical solution of the relativistic Schrödinger equation.

What is the reason for this discrepancy δ? It could signify either a deficiency in the nuclear densities or a difficulty with the reaction theory. With regard to the nuclear densities it should be recalled that the Hartree-Fock density is only an approximate representation of the proton distribution. Although the DME theory is generally in agreement with electron-scattering and μ-atom experiments, significant fluctuations about the mean field densi-

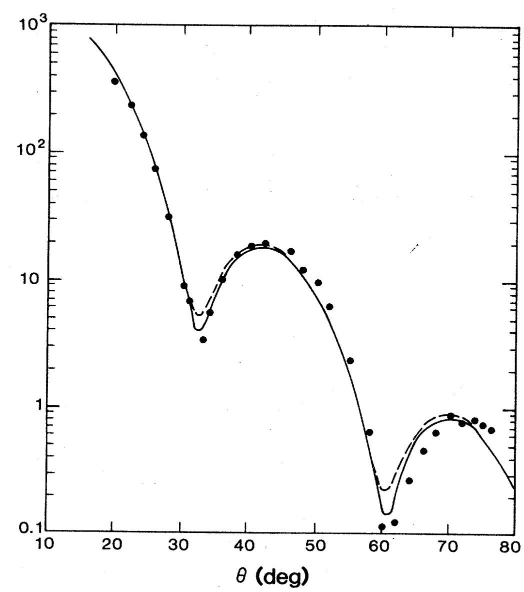

FIG. 3. Elastic scattering of π^+ mesons from ^{40}Ca. The solid curve is an optical-model calculation using the theory of Ref. 5(b) with second-order corrections taken from Ref. 17. Data are from Ref. 15(b). The dashed curve includes the Coulomb energy shift in Eq. (13).

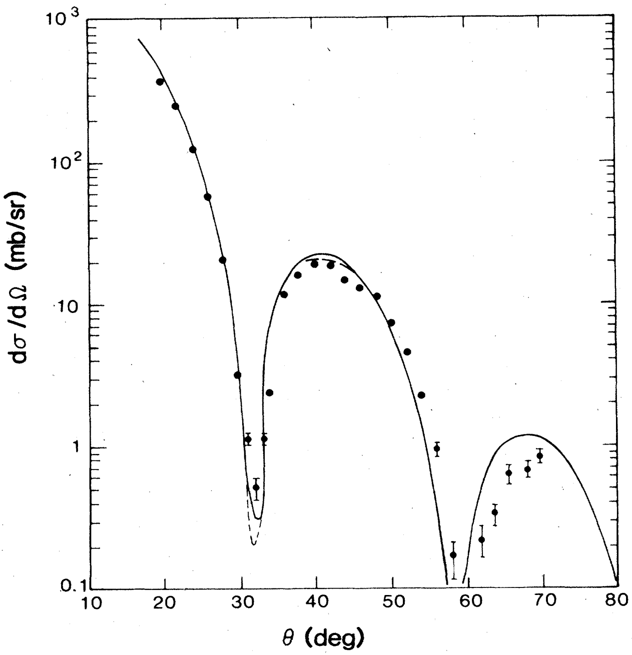

FIG. 4. Elastic scattering of π^- mesons from ^{40}Ca. Solid and dashed curves are calculated as in Fig. 3. Data are from Ref. 15(b).

ty could occur in the nuclear surface,[30] the region of the nucleus to which 180-MeV pion scattering is most sensitive. However, these fluctuations *increase* the density in the surface, and cannot therefore be the source of the discrepancy δ.

The values of Y obtained from the free pion-nucleon scattering amplitude using Eq. (11) are compared to the empirical values in Table V. One notices that the latter are considerably smaller than the theoretical values of Y. This means that the depths of the minima in the lowest-order optical-model theory will be too shallow. Because of the sensitivity of the quantity Y to the real part of the scattering amplitude *in the medium*, this discrepancy is a particularly good indicator of medium modifications to the Δ_{33} resonance.

Thus the discrepancies in b_1 and Y presumably reflect the need for medium modifications to the pion-nucleon amplitude. There are many possible sources for these corrections in the theory,[5(a)] and these are not yet completely sorted out. However, the corrections have been determined phenomenologically[17] in terms of the second-order optical potential $U^{(2)}$ using an analysis of the extensive data set on elastic scattering, SCX, and double-charge exchange (DCX) at 164 MeV. This theory incorporates a lowest-order optical potential derived from free pion-nucleon scattering and a second-order optical potential whose form is derived from theory and specified in terms of a few parameters. The position of the Δ_{33} resonance was found to be shifted by 35 MeV in the medium, presumably by kinematic and dispersive effects of the medium. The theory demonstrates that one set of parameters characterizes the pion-nucleus interaction throughout the periodic table in terms of the neutron and proton densities. As it is important in Sec. V to have an optical-potential theory that correctly describes the scattering from the calcium isotopes at 180 MeV, we examine next how well the second-order optical potential determined at 164 MeV in Ref. 17 describes the 180-MeV calcium data.

Extension of the eikonal theory to include $U^{(2)}$ is possible.[5(b)] However the theory becomes quite complicated in this case and for our present purposes we solve the Klein-Gordon equation directly. We show in Figs. 3—6 the elastic scattering of $\pi^{\pm}$ from ^{40}Ca and ^{48}Ca. Figures 3 and 4 show that the scattering data are well reproduced by the second-order parameters[17] for ^{40}Ca. Skyrme III densities[31] were used for the calculation. The dashed curve shows the effect of the Coulomb energy shift of the lowest-order optical potential evaluated according to the prescription in Eq. (13). The effect of the Coulomb force

TABLE V. Values of Y compared to theory.

Isotope	Pion	Y (exp)	Y^a
^{40}Ca	π^+	-0.12	-0.32
	π^-	-0.11	-0.53
^{42}Ca	π^+	-0.12	-0.33
	π^-	-0.08	-0.46
^{44}Ca	π^+	-0.12	-0.33
	π^-	-0.09	-0.55
^{48}Ca	π^+	-0.09	-0.35
	π^-	-0.08	-0.58

[a]Solution of Eq. (11), with Wallace.

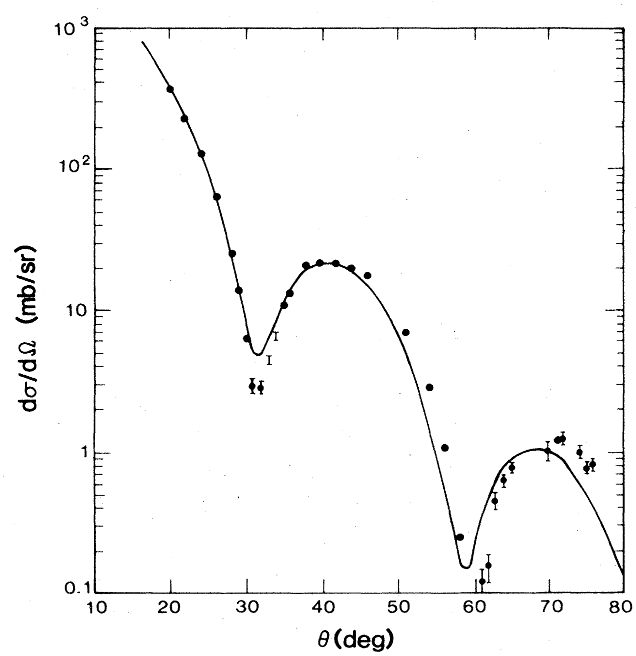

FIG. 5. Elastic scattering of π^+ mesons from ^{48}Ca. Solid curve is calculated as in Fig. 3. Data are from Ref. 15(b).

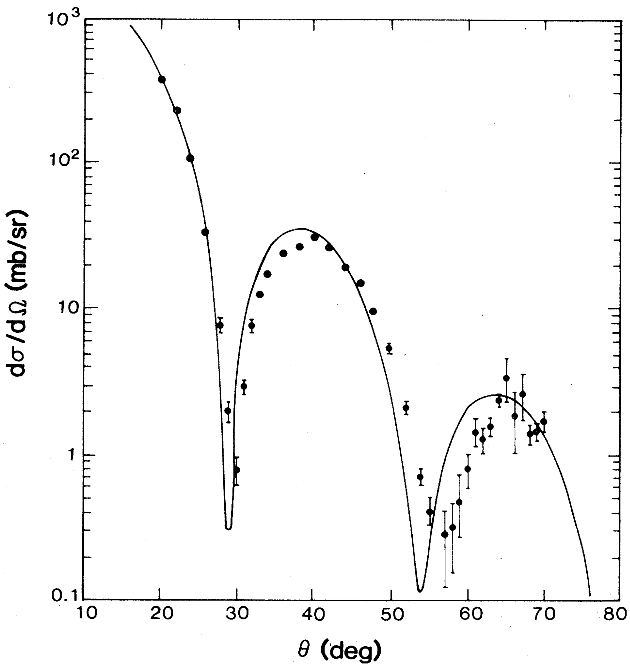

FIG. 6. Elastic scattering of π^- mesons from ^{48}Ca. Solid curve is calculated as in Fig. 3. Data are from Ref. 15(b).

is small, but the trend of the theory is opposite to that of the data. Thus the data are better described without the correction in Eq. (13), and one understands why phenomenological descriptions[32] often neglect this term. We expected the correction in Eq. (13) to be a good approximation[22,33] to the Coulomb modification to the strong interaction and do not understand why the data do not reflect it. Figures 5 and 6 show $\pi^\pm$ scattering from ^{48}Ca. Again, the optical-model theory with medium modifications is seen to reproduce the data very nicely. The main discrepancies are in the depths of the minima for π^+ scattering and the shift of the theoretical angular distributions toward smaller angles, particularly noticeable in the case of π^- scattering from ^{48}Ca.

The residual discrepancy between theory and experiment at 180 MeV in Figs. 3–6 is to some extent due to the fact that we used the parameters of the second-order optical potential determined at 164 MeV. However, there is also a strong sensitivity to the nuclear densities, and the discrepancies may also, in part, be of this origin. One of the main purposes of this paper is to see to what extent different densities could lead to improved results. Because the diffraction theory faithfully reproduces the sensitivity of the optical-model theory[11] to changes in density we will next use the data in conjunction with the analytical eikonal theory to study this sensitivity.

V. NEUTRON DENSITY IN THE CALCIUM ISOTOPES

One of the most tantalizing prospects of the use of pion-nucleus scattering data has been to probe the details of nuclear wave functions, especially of the neutrons. Because the π^- interacts more strongly with neutrons than π^+ in the resonance region, it is possible in principle to extract information about neutron densities from elastic and total cross-section data. There have been several attempts to do this.[12,13] However, these analyses had the drawback that the pion optical potential was taken purely from theoretical models. Recent studies of pion SCX have been made and these data are beginning to provide a phenomenological characterization of the isovector pion-nucleus interaction, which is needed to justify the procedures used. The analysis of Ref. 17 found a large correction to the isovector optical potential and a moderately small correction to the isoscalar optical potential. We can estimate the size of the corrections to U by dropping the less important Laplacian and s-wave terms to find[5]

$$-\frac{U}{k^2}\cong\left[\lambda_0^{(1)}+\lambda_0^{(2)}\frac{\rho}{\rho_0}\right]\rho-\frac{\epsilon_\pi}{2}\left[\lambda_1^{(1)}+\lambda_1^{(2)}\frac{\rho}{\rho_0}\right]\Delta\rho\ . \tag{27}$$

The imaginary part of U is most important in determining b_1 [see Eqs. (7) and (8)], and at the self-consistent point $\rho(b_1)/\rho_0\approx 0.1$. Taking into account the 35-MeV energy shift presumably arising from isobar propagation and using the λ values of Ref. 17, we find

$$\mathrm{Im}(\lambda_0^{(1)}+\lambda_0^{(2)}\rho/\rho_0)/\mathrm{Im}\lambda_0^{(1)}=1.06 \tag{28}$$

and

$$\mathrm{Im}(\lambda_1^{(1)}+\lambda_1^{(2)}\rho/\rho_0)/\mathrm{Im}\lambda_1^{(1)}=1.29\ . \tag{29}$$

These are only estimates because we have not included the Wallace corrections or the Laplacian terms that will slightly modify the strength of the isoscalar and isovector terms. Because the ratios differ significantly from 1 (especially for the isovector strength), the medium modifications must be taken into account in an analysis to obtain neutron densities.

In our analysis the main interest is to study the effect of the large renormalization in Eqs. (28) and (29). There is some minor nucleus dependence to the renormalized strength arising from the fact that $\rho(\bar{b})$ and the Laplacian terms vary through the calcium isotopes, but we shall ignore these. Thus, we take $U(\bar{b})$ to have the following form

$$-\frac{U(\bar{b})}{k^2}=\tilde{\lambda}_0^{(1)}\rho(\bar{b})-\epsilon_\pi\tilde{\lambda}_1^{(1)}\Delta\rho(\bar{b})\ , \tag{30}$$

where $\tilde{\lambda}_0^{(1)}$ and $\tilde{\lambda}_1^{(1)}$ are taken to be constant throughout the calcium isotopes. As we shall see below, our results are sensitive to the scattering dynamics only via the ratio

$$\gamma\equiv\tilde{\lambda}_1^{(1)}/\tilde{\lambda}_0^{(1)}\ . \tag{31}$$

The estimate in Eqs. (28) and (29) for 164 MeV gives $\gamma=1.22$ instead of the free value $\gamma=1.0$. In this paper we need the value of γ for 180 MeV pions. We present below a simple procedure to determine it directly from the data.

For our study of neutron distributions, we will relate the variation of the parameter b_1 through the calcium isotopes to the separate variation of the neutron and proton

TABLE VI. Values of β_i determined from experiment (Eq. 34). Statistical errors are of the order of a few percent.

Isotope	Pion	β
^{48}Ca	π^+	1.14
	π^-	1.57
^{44}Ca	π^+	1.08
	π^-	1.26
^{42}Ca	π^+	1.03
	π^-	1.12

densities. This may be accomplished by noticing that Eq. (7) defining b_1 is identical for all isotopes. Then using the explicit form of Eq. (8) for $X(b)$ gives a condition which relates b_1 and a to the imaginary part of the optical potential:

$$\sqrt{a^{40}b_1^{40}}\;\mathrm{Im}\,U^{40}(b_1^{40})=\sqrt{a^i b_1^i}\;\mathrm{Im}\,U^i(b_1^i)\;, \tag{32}$$

where a^i is the $1/e$ falloff distance from b_1^i of U. Equation (32) allows us to evaluate $\mathrm{Im}\,U^i$ in the surface of the nucleus from the numbers in Table I. It is more revealing to compare U at a common point in the nucleus $\bar{b}_1$, and in order to do this we write Eq. (32) as follows

$$\frac{\mathrm{Im}\,U^i(\bar{b}_1)}{\mathrm{Im}\,U^{40}(\bar{b}_1)}=\left[\frac{a^{40}b_1^{40}}{a^i b_1^i}\right]^{1/2}\frac{\mathrm{Im}\,U^{40}(b_1^{40})}{\mathrm{Im}\,U^{40}(\bar{b}_1)}\,\frac{\mathrm{Im}\,U^i(\bar{b}_1)}{\mathrm{Im}\,U^i(b_1^i)}\equiv\beta_i\;. \tag{33}$$

We choose $\bar{b}_1=4.7$ fm. We have assumed that the densities fall exponentially in a small region of the surface in the vicinity of $\bar{b}$, according to Eq. (9). The ratios on the right-hand side of Eq. (33) may then be entirely determined from the information in Table I,

$$\beta_i=\left[\frac{a^{40}b_1^{40}}{a^i b_1^i}\right]^{1/2}\frac{e^{(\bar{b}_1-b_1^{40})/a^{40}}}{e^{(\bar{b}_1-b_1^i)/a^i}} \tag{34}$$

and the results are given in Table VI. The quantities a in Eqs. (33) and (34) refer to a_0, whereas the a in Table I are related to a_0 by Eq. (10). We take a_0 to be the same as a in evaluating Eq. (34). This does not lead to significant errors because the correction, given in Eq. (10), is small with little variation among the calcium isotopes. The b_1 in Eq. (33) are actually the Coulomb-corrected b_1, evaluated according to Eq. (12), but because we evaluate the β_i for π^+ and π^- separately, these Coulomb corrections may be ignored.

We now want to solve the left-hand side of Eq. (33) for $\rho_n^i(\bar{b}_1)$ and $\rho_p^i(\bar{b}_1)$, i.e.,

$$\frac{\mathrm{Im}\,U^i(\bar{b}_1,\pi^+)}{\mathrm{Im}\,U^{40}(\bar{b}_1,\pi^+)}=\beta_i(\pi^+) \tag{35}$$

and

$$\frac{\mathrm{Im}\,U^i(\bar{b}_1,\pi^-)}{\mathrm{Im}\,U^{40}(\bar{b}_1,\pi^-)}=\beta_i(\pi^-)\;. \tag{36}$$

For U we use Eq. (30) and express results in terms of γ defined in Eq. (31). Taking γ to be constant throughout the calcium isotopes, we find

$$\rho_p^i/\rho_p^{40}=\frac{1}{2\gamma}\left[\beta_+(1+\gamma/2)^2-\beta_-(1-\gamma/2)^2-(1+\gamma/2)(1-\gamma/2)(\beta_--\beta_+)\frac{\rho_n^{40}}{\rho_p^{40}}\right], \tag{37}$$

$$\rho_n^i/\rho_n^{40}=\frac{1}{2\gamma}\left[\beta_-(1+\gamma/2)^2-\beta_+(1-\gamma/2)^2+(1+\gamma/2)(1-\gamma/2)(\beta_--\beta_+)\frac{\rho_p^{40}}{\rho_n^{40}}\right]. \tag{38}$$

To the extent that the proton density in nuclei is well described by the Hartree-Fock theory, Eq. (37) determines γ phenomenologically. Once γ is known, Eq. (38) can be used to determine the variation of the neutron density through the isotopes of calcium in the surface. We use the measured charge-exchange cross sections as an independent check on our results.

To evaluate γ from Eq. (37) we take ρ_n/ρ_p for ^{40}Ca from the DME theory, $\rho_n/\rho_p=0.941$. Whereas this ratio is model dependent, it occurs in a relatively minor correction. We need also as input the ratio of ρ_p^{48}/ρ_p^{40} at $r=4.7$ fm. The proton densities have been accurately determined from electron scattering and μ^--atom measurements.[34] We find

$$\rho_p^{48}(4.7)/\rho_p^{40}(4.7)=1.03 \tag{39}$$

and from Eq. (37) we find $\gamma=1.3$. This is just a bit larger than the estimate $\gamma=1.22$ using Eqs. (28) and (29) at 164 MeV. Using this value of γ and the ρ_n^{40}/ρ_p^{40} from the Negele-Vautherin[28] DME theory, we find the values of ρ^i/ρ^{40} for neutrons and protons given in Tables VII and VIII.

Table VII indicates the sensitivity of the extracted densities to the isospin-dependent corrections in $U^{(2)}$. Table VII (top half) gives the results for protons. In the first column are the ratios $\rho_p(i)/\rho_p(40)$ evaluated on the basis of analysis of μ^--atom data taken at LAMPF and electron scattering data. These numbers are the "exact" results to which the pion-scattering data must be compared. The second column gives the results of the full analysis including $U^{(2)}$. The pion results compare to within $\pm 5\%$, which is an index of how seriously we should take the neutron-density results. The third column in Table VII

TABLE VII. Effects of adding U^2.

i	μ atom[a]	ρ_p^i/ρ_p^{40} at $r=4.7$ fm $\pi+$ nucleus	$\pi+$ nucleus (no $U^{(2)}$)
^{48}Ca	1.03	1.03	0.93
^{44}Ca	1.08	1.03	0.93
^{42}Ca	1.05	1.01	0.99

i	p+nucleus[b]	ρ_n^i/ρ_n^{40} at $r=4.7$ fm $\pi+$nucleus	$\pi+$nucleus (no $U^{(2)}$)
^{48}Ca	1.80	1.69	1.80
^{44}Ca	1.46	1.31	1.35
^{42}Ca	1.24	1.15	1.17

[a]Reference 34.
[b]Reference 35.

(top half) shows what we get by turning off the isospin-dependent pieces of $U^{(2)}$, i.e., by putting $\gamma=1$ in Eqs. (28) and (29). There is a 10% decrease in the values for ^{48}Ca, and this verifies the importance of $U^{(2)}$ for making a detailed assessment of the densities from pion elastic scattering.

In Table VII (bottom half) we show the importance of $U^{(2)}$ for the neutron densities. The first column shows the ratio ρ_n^i/ρ_n^{40} calculated from the results of an analysis[35] of proton-nucleus scattering. The second column is our analysis of the π-nucleus scattering data. The pion ratios are consistently below the proton-scattering results by 5–10%. Note that adding $U^{(2)}$ has a smaller effect on the neutrons than it has on the protons and that it makes the disagreement with the proton-scattering analysis even greater.

Table VIII compares various models and the empirical analyses of proton and neutron densities. The protons are compared in Table VIII (top half). The first two columns are the same as those in Table VII (top half) and the last two are theoretical predictions of the Negele-Vautherin[28] and SKIII (Ref. 31) Hartree-Fock theories. There is reasonably good agreement. In Table VIII (bottom half), for neutrons, we again reproduce the first two columns of Table VII (bottom half). The last two show the Hartree-Fock densities. The middle column labeled "scaled" is the result that would be obtained in the absence of a neutron halo; i.e., the neutron and proton densities were assumed to be everywhere proportional to N/Z. One sees that the analysis of the pion-scattering experiment confirms the existence of a neutron halo, but that the halo is not as pronounced as in the Hartree-Fock theories.

One might be more comfortable with the analysis at 180 MeV after comparing the theory to pion charge-exchange data. This is done in Fig. 7. The data[16] are as yet preliminary, but the figure shows that by including the isospin-dependent terms in $U^{(2)}$, we improve the reproduction of the single-charge-exchange data. For this calculation we used the Negele-Vautherin DME Hartree-Fock densities. It is pleasing that the same corrections in $U^{(2)}$ lead to a simultaneous improvement in theory for the elastic and the SCX data. Within the same approximations which lead to Eqs. (1)–(11) the pion single-charge-exchange cross section at 0° reads[36]

$$\left[\frac{d\sigma}{d\Omega}(0^\circ)\right]_{\mathrm{SCX}}=\frac{1}{2(N-Z)}\left\{\gamma akR\frac{\Delta\rho}{\rho}[1-0.577(a_\rho/a_{\Delta\rho}-1)]\right\}^2, \tag{40}$$

where a and R denotes the average value for π^+ and π^- scattering. The value of $\Delta\rho/\rho$ has to be evaluated at the self-consistency point $\bar{b}_1$. The factor within square brackets takes into account the different rate of falloff for ρ and $\Delta\rho$. Equation (40) reproduces approximately the "exact" results of Fig. 7, which were obtained by solving numerically the Klein-Gordon equation. Our type of analysis of π^+/π^- elastic scattering differential cross sections can therefore easily be tested against the single charge exchange cross sections.

We have also compared our results to the Hartree-Fock-Bogoliubov calculations of Dechargé and Gogny.[37] We find theoretical values intermediate between the Negele DME and SKIII results, except for ρ_n^{42}/ρ_n^{40}, which are slightly larger than the DME results in Table VIII.

TABLE VIII. Comparison to Hartree-Fock theory.

i	μ atom	ρ_p^i/ρ_p^{40} at $r=4.7$ fm $\pi+$N	DME[a]	SKIII[b]
^{48}Ca	1.03	1.03	1.06	1.15
^{44}Ca	1.08	1.03	1.03	1.07
^{42}Ca	1.05	1.01	1.01	1.04

i	p+N	ρ_n^i/ρ_n^{40} at $r=4.7$ fm $\pi+$N	Scaled	DME[a]	SKIII[b]
^{48}Ca	1.78	1.69	1.44	1.88	2.01
^{44}Ca	1.46	1.31	1.29	1.43	1.48
^{42}Ca	1.24	1.15	1.15	1.21	1.17

[a]Reference 28.
[b]Reference 31.

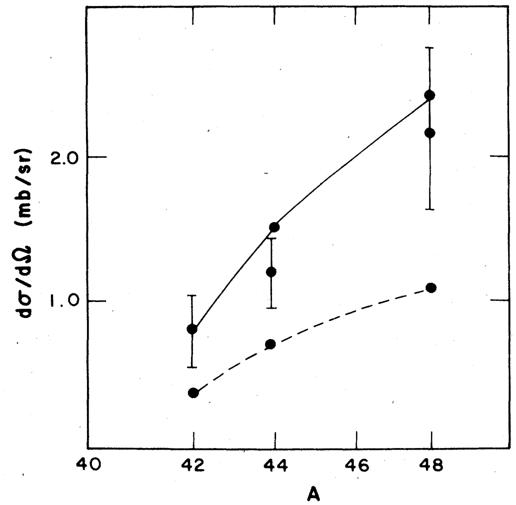

FIG. 7. Pion single-charge exchange from the calcium isotopes. The dashed curve is the theory of Refs. 5(b) and 17 without isospin-dependent terms in $U^{(2)}$; the solid curve includes the full $U^{(2)}$. The data are from Ref. 16.

VI. SUMMARY AND CONCLUSIONS

We have shown that resonance-energy pion-nucleus elastic scattering is well described at small-momentum transfer ($q \lesssim 1.15$ fm^{-1}) by the analytical theory of Ref. 11, including Coulomb effects. This theory parametrizes the data in terms of three numbers: a diffuseness a, a strong absorption radius b_1, and a ratio of real-to-imaginary components of the optical potential Y.

We compared the empirical quantities a, b_1, and Y to values obtained from a theoretical model that builds the potential from realistic densities and the free pion-nucleon-scattering amplitude. Qualitative reproduction of the empirical results was obtained for a and b_1, but the necessity of making corrections for isobar propagation and interaction was observed in trying to understand Y. It was shown that the optical potential previously determined for 165-MeV pion elastic scattering also worked well at 180 MeV, giving confidence in the underlying optical model. Small anomalies in the Coulomb modification of the strong interaction are not understood.

Having come to a phenomenological understanding of the scattering dynamics, we used the theory to examine the neutron and proton densities in the calcium isotopes. By examining the variation of b_1 for $\pi^{\pm}$ scattering and using empirically determined strengths for the isovector and isoscalar optical potentials, we deduced values for $\rho^{A}_{n(p)}(\bar{b}_1)/\rho^{40}_{n(p)}(\bar{b}_1)$, the ratio of neutron (proton) densities in the surface of ^{A}Ca compared to that in ^{40}Ca. The proton densities compared favorably to the empirical densities, and the neutron densities showed evidence of a neutron halo. Comparison to Hartree-Fock densities revealed that there is nearly as much spread among the different Hartree-Fock theories as there is between the empirical and Hartree-Fock densities.

Making use of the Hartree-Fock densities, we made predictions for single charge exchange at 180 MeV. We found that the theory predicts too little charge exchange unless the isovector interaction is substantially enhanced, consistent with the analysis at 165 MeV. The enhanced isovector interaction was important for obtaining the empirical Hartree-Fock proton density in ^{48}Ca.

Previous analyses of pion-scattering data to obtain neutron densities have been criticized[38] because the variation of the optical potential throughout the isotopes that was used in the analysis had not been tested empirically. We have based the results of this paper on a theoretically derived optical potential[5] that has been shown[17] to scale throughout the periodic table in a manner consistent with the elastic and charge-exchange data.

It is of interest to understand the extent to which the discrepancies between theory and experiment in the densities of Table VII are due to the Hartree-Fock theory and due to the scattering theory. An improved analysis of the scattering data could be made by working directly with the solution of the Klein-Gordon equation rather than the eikonal theory. A procedure similar to that of Ref. 35 could lead to an assignment of errors on the density distribution. It would be interesting to make an analysis at a variety of energies; the strong energy dependence of the pion-nucleon amplitude would permit different regions of the nucleus to be explored at the different energies. Having the charge exchange *and* elastic scattering available would be important to fix the isovector terms in the optical potential.

One should not expect to reproduce in detail the results of the Hartree-Fock theory. This is clear because of the variation in the predictions of the different effective interactions. Perhaps even more significant would be the fluctuations about the mean-field densities recently discussed in Ref. 30. A striking discrepancy between electron-scattering results on ^{206}Pb/^{205}Tl and the mean-field predictions has been observed[39] for the $3S$ orbit and attributed to corrections of this origin. Eventually theoretical models that combine the nuclear structure and reaction theory at a deeper level may lead to useful insight. Development of momentum-space methods that may be capable of handling such extensions are under way.[7,8]

ACKNOWLEDGMENTS

We acknowledge helpful discussions with H. A. Bethe and thank E. R. Siciliano for providing us with the Skyrme III densities. Research was supported in part by the Swiss National Science Foundation (J.-F.G.) and the U. S. Department of Energy [(M.B.J.) and (J.A.J.)].

*Present address: Physics Division, Argonne National Laboratory, Argonne, IL 60439.

[1]K. Stricker, H. McManus, and J. A. Carr, Phys. Rev. C **19**, 929 (1979); K. Stricker, J. A. Carr, and H. McManus, *ibid*. **22**, 2043 (1980).

[2]M. Hirata, J.-H. Koch, F. Lenz, and E. J. Moniz, Ann. Phys. (N.Y.) **120**, 205 (1979); E. Oset and W. Weise, Phys. Lett. **B77**, 159 (1978); K. Klingenbeck, M. Dillig, and M. G. Huber, Phys. Rev. Lett. **41**, 387 (1978).

[3]L. C. Liu and C. M. Shakin, Phys. Rev. C **19**, 129 (1979); L. C. Liu, *ibid*. **27**, 1611 (1983).

[4]W. B. Kaufmann and W. R. Gibbs, Phys. Rev. C **28**, 1286 (1983).

[5](a) M. B. Johnson and E. R. Siciliano, Phys. Rev. C **27**, 730 (1983); (b) M. B. Johnson and E. R. Siciliano, *ibid*. **27**, 1647 (1983).

[6]R. A. Freedman, G. A. Miller, and E. M. Henley, Phys. Lett. **103B**, 397 (1981); Nucl. Phys. **A389**, 457 (1982).

[7]D. J. Ernst, G. A. Miller, and D. L. Weiss, Phys. Rev. C **27**, 2733 (1983); D. J. Ernst and M. B. Johnson, Phys. Rev. C (to be published).

[8]J. Johnstone (unpublished).

[9]C. Schmidt, Nuovo Cimento Lett. **4**, 459 (1970); C. Wilkin, *ibid*. **4**, 491 (1970).

[10]R. T. Glauber, *Lectures in Theoretical Physics* (Interscience, New York, 1959), Vol. I, p. 315.

[11]J.-F. Germond and M. B. Johnson, Phys. Rev. C **22**, 1622 (1980).

[12]M. K. Jakobson, G. R. Burleson, J. R. Calarco, M. D. Cooper, D. C. Hagerman, I. Halpern, R. H. Jeppesen, K. F. Johnson, L. D. Knutson, R. E. Marrs, H. O. Meyer, and R. P. Redwine, Phys. Rev. Lett. **38**, 1201 (1977).

[13]M. B. Johnson and H. A. Bethe, Comments Nucl. Part. Phys. **8**, 75 (1978).

[14]P. Gretillat, J.-P. Egger, J.-F. Germond, C. Lunke, E. Schwarz, C. Perrin, and B. Preedom, Nucl. Phys. **A364**, 270 (1981).

[15](a) Chris Morris and K. Boyer, private communication; (b) K. Boyer, Ph.D. thesis, University of Texas, Austin, 1983 (unpublished). Two different analyses of the same experiment are shown in this paper, but the results are identical.

[16]H. Baer, J. D. Bowman, and F. H. Cverna, Los Alamos National Laboratory Report LA-8994-PR, 1983, p. 30.

[17]S. J. Greene, C. J. Harvey, P. A. Seidl, R. Gilman, E. R. Siciliano, and M. B. Johnson, Phys. Rev. C **30**, 2003 (1984).

[18]W. E. Frahn, Institut de Physique Nucleaire Orsay Report IPNO-TH-80-44, 1980.

[19]R. D. Amado, J.-P. Dedonder, and F. Lenz, Phys. Rev. C **21**, 647 (1980).

[20]M. Bleszynski, R. J. Glauber, and P. Osland, Phys. Lett. **B104**, 389 (1981).

[21]E. V. Inopin and Yu. A. Berezhnoy, Nucl. Phys. **63**, 689 (1965).

[22]J.-F. Germond and C. Wilkin, Ann. Phys. (N.Y.) **121**, 285 (1979).

[23]M. D. Cooper and M. B. Johnson, Nucl. Phys. **A260**, 352 (1976); M. D. Cooper, M. B. Johnson, and G. B. West, *ibid*. **A292**, 350 (1977).

[24]R. H. Jeppesen, M. J. Jakobson, M. D. Cooper, D. C. Hagerman, M. B. Johnson, R. P. Redwine, G. R. Burleson, K. F. Johnson, R. E. Marrs, H. O. Meyer, I. Halpern, and L. D. Knutson, Phys. Rev. C **27**, 697 (1983).

[25]Note the special meaning of b_1 in Eqs. (17) and (18).

[26]S. J. Wallace, Ann. Phys. (N.Y.) **78**, 190 (1973).

[27]Q. Ingram, E. Boschitz, L. Pflug, J. Zichy, J. P. Albanèse, and J. Arvieux, Phys. Lett. **76B**, 173 (1978).

[28]J. W. Negele and D. Vautherin, Phys. Rev. C **5**, 1472 (1972).

[29]B. Zeidman, LAMPF Users Newsletter **13**, 91 (1981); private communication.

[30]H. Ebensen and G. F. Bertsch, Phys. Rev. C **28**, 355 (1983); Z. Y. Ma and J. Wambach, Nucl. Phys. **A402**, 275 (1983).

[31]M. Beiner, H. Flocard, N. Van Giai, and P. Quentin, Nucl. Phys. **A238**, 29 (1975).

[32]J. Fröhlich, H. Pilkuhn, and H. G. Schlaile, Nucl. Phys. **A415**, 399 (1984); Phys. Lett. **121B**, 235 (1983).

[33]J. Johnstone (unpublished).

[34]H. D. Wohlfahrt, E. B. Shera, M. V. Hoehn, Y. Yamazaki, G. Fricke, and R. M. Steffen, Phys. Lett. **73B**, 131 (1978).

[35]L. Ray, G. W. Hoffman, M. Barlett, J. McGill, J. Amann, G. Adams, G. Pauletta, M. Gazzaly, and G. S. Blanpied, Phys. Rev. C **23**, 828 (1981).

[36]M. B. Johnson, Phys. Rev. C **22**, 192 (1980).

[37]J. Dechargé and D. Gogny, Phys. Rev. C **21**, 1568 (1980); L. Ray, private communication.

[38]M. M. Sternheim and K. B. Yoo, Phys. Rev. Lett. **41**, 1781 (1978).

[39]B. Frois, J. M. Cavedon, D. Goutte, M. Huet, Ph. Leconte, C. N. Papanicolas, X.-H. Phan, S. K. Platchkov, S. E. Williamson, W. Boeglin, and I. Sick, Nucl. Phys. **A396**, 409 (1983).